Cr^+ (and Fe^+–Cu^+) ions afford M(HNCO)(alkene)$^+$ complexes in the secondary reactions if a tertiary isocyanate is involved. This conclusion is also supported by the data in Table XI which show that, in contrast to the secondary isocyanates, eqs 16, 18, and 23 are observed for Cr^+ in the case of the tertiary substrates **3** and **4**.

The preceding observations should caution researchers employing sector-field instruments where an ion with an elemental composition corresponding to the adduct complex is selected as precursor for MI or CID studies. These ions are usually formed in chemical ionization (CI) sources by electron impact on a mixture of the substrate and a volatile organometallic complex such as $Fe(CO)_5$. The adduct complex is believed to be formed by simple ligand exchange from $Fe(CO)^+$, for instance. As the present study shows, what appears to be a simple ligand-exchange reaction is not necessarily one. Although, admittedly, the FTICR conditions differ from the high-pressure CI plasma, the occurrence of similar processes would ultimately lead to false conclusions if a dissociated complex was selected from the ion source and erroneously taken to be an intact adduct complex.

Note Added in Proof. The reaction of Na^+ and K^+ with **2** has now been studied but was found to afford only adduct complexes with a very slow rate. MI spectra of *s*-BuNCOH$^+$, formed with H_2 or *i*-C_9H_{10} CI plasma, result in the exclusive loss of [HNCO]. The latter experiment was done in a four-sector BEBE instrument and the result is completely in line with the known proton affinity of (*E*)-2-butene (PA = 750 kJ mol^{-1})[50] and the estimated value for NCOH (PA ≈ 722 kJ mol^{-1}).[51] The MI spectrum of protonated **2a** accordingly results in loss of [HNCO] only (100%) with any [DNCO] loss being significantly less than 3%, the limit of detectability in this particular experiment.

Acknowledgment. We gratefully acknowledge the continuous financial support of our work by the Deutsche Forschungsgemeinschaft, the Fonds der Chemischen Industrie, and the Volkswagen-Stiftung.

Registry No. 1, 1795-48-8; **2**, 15585-98-5; **3**, 1609-86-5; **4**, 1612-71-1; Cr^+, 14067-03-9; Mn^+, 14127-69-6; Fe^+, 14067-02-8; Co^+, 16610-75-6; Ni^+, 14903-34-5; Cu^+, 17493-86-6; Zn^+, 15176-26-8; D_2, 7782-39-0.

(49) In the case of Fe^+ reacting with **4a**, we were unable to detect the d_2- and d_4-labeled "adduct complexes" owing to their low intensity and the occurrence of isobaric $FeC_8H_{16-x}D_x^+$ ions formed in the reactions of $FeC_3H_{6-y}D_y^+$ with **4a**. The observation of d_5-, d_6-, and d_7-labeled "adducts" in the case of **4b**, however, unambiguously proves that for *t*-PentNCO too, Fe(HNCO)(alkene)$^+$ complexes are formed for Fe^+. For all other metal ions the labeling distributions with **4a** and **4b** were established and found to be according to the expectations.

(50) Lias, S. G.; Liebman, J. F.; Levin, R. D. *J. Phys. Chem., Ref. Data No. 3* **1984**, 695.

(51) Estimated from the known[52,53] PA(HNCO) = 759 kJ mol^{-1}, the calculated[53] energy difference of 79 kJ mol^{-1} between the resulting H_2NCO^+ ion and $HNCOH^+$, and the known difference in heat of formation between HNCO and HOCN ($\Delta\Delta H_f^\circ$ = 42 kJ mol^{-1}).[54]

(52) Wight, C. A.; Beauchamp, J. L. *J. Phys. Chem.* **1980**, *84*, 2503.

(53) Hop, C. E. C. A.; Holmes, J. L.; Ruttink, P. J. A.; Schaftenaar, G.; Terlouw, J. K. *Chem. Phys. Lett.* **1989**, *156*, 251.

(54) Shaw, R. In *The Chemistry of Cyanates and their Thio Derivatives*; Patai, S., Ed.; Wiley-Interscience: Chichester, 1977; p 237.

Characterization of Hydrogen Bonding in Zeolites by Proton Solid-State NMR Spectroscopy

Jeffery L. White, Larry W. Beck, and James F. Haw*

Contribution from the Department of Chemistry, Texas A&M University, College Station, Texas 77843. *Received July 8, 1991*

Abstract: Variable-temperature magic-angle spinning proton NMR spectroscopy has characterized the structure and dynamics of hydrogen-bonded adsorption complexes between various adsorbates and the Bronsted acid site in a representative zeolite, H-ZSM5. The active site Bronsted proton chemical shift was found to be extremely sensitive to the amount and type of adsorbate introduced. The adsorbates studied were acetylene, ethylene, carbon monoxide, benzene, ethane, and nitrogen, with emphasis on the first four. Slow-exchange spectra obtained at 123 K for loadings of less than 1 equiv showed resolved peaks for free and complexed Bronsted sites. Low-temperature reverse cross-polarization experiments confirm that the adsorbates hydrogen-bond specifically to the Bronsted site and do not interact with the external silanol groups. Fast-exchange-averaged chemical shifts were observed at 298 K. Quantitative treatment of the loading-dependent chemical shifts for acetylene, ethylene, and carbon monoxide yielded equilibrium constants at 298 K of ca. 7, 7, and 0.7 equiv^{-1}, respectively. The differences in the observed change in chemical shift with type of adsorbate are explained in terms of hydrogen-bond shifts and established theories of shielding contributions from neighboring group anisotropy effects. A semiquantitative treatment of induced shifts for acetylene, ethylene, and benzene adsorption yielded a characteristic hydrogen-bond distance ranging from 2.35 to 2.78 Å, which is in agreement with gas-phase model compounds and only slightly larger than distances calculated for model clusters using quantum chemical methods. These results suggest that quantitative interpretation of proton chemical shifts for zeolite catalysts provides information on the strength of hydrogen bonds and suggests geometries of the hydrogen-bonded complexes similar to those observed in the gas phase and calculated for model clusters. Furthermore, benzene undergoes rapid deuterium–hydrogen exchange near 298 K, apparently through a hydrogen-bonded intermediate.

Introduction

There is considerable interest in the properties of Bronsted acid sites in zeolite catalysts and their interactions with various adsorbed molecules.[1] The locus of catalytic activity in zeolites is an acidic hydrogen attached to a bridging framework oxygen site within the zeolite channels. Several approaches have been used in attempting to more clearly understand the chemistry that occurs within the zeolite channels at the active site. The most common methods involve either calorimetric or spectroscopic techniques.[1] Enthalpies of adsorption and desorption for bases such as amines are used to measure the apparent strength of interaction and thus provide a measure of some function of catalyst acidity.[2] However,

* Author to whom correspondence should be addressed.

(1) Rabo, J. A.; Gajda, G. J. *Catal. Rev.-Sci. Eng.* **1989–90**, *31*, 385.

(2) Jacobs, P. A. In *Characterization of Heterogeneous Catalysts*; Dellanay, F., Ed.; Marcel Dekker: New York, 1984.

0002-7863/92/1514-6182$03.00/0

these methods may be complicated by diffusional constraints and multiple adsorption/desorption processes. One of the earliest and most widely used techniques for the study of zeolites is infrared spectroscopy.[3] Here, both the position of the hydroxyl stretching absorbance band and the position of absorbance bands from probe molecules such as pyridine are used to probe both acidity and the nature of interaction.[2] Recently, magic-angle spinning (MAS) ^{1}H solid-state NMR studies of several zeolites have clearly resolved Bronsted acid site protons from surface silanol groups and nonframework (external) hydroxyl groups.[4,5] Since protons are chemically dilute spins in zeolites, proton NMR spectra do not require multiple-pulse averaging, and useful resolution may be obtained with MAS only, both in the absence and presence of adsorbates. Recently, it was reported that methanol forms extended hydrogen-bonded networks with the Bronsted protons in zeolite H-ZSM5.[6] Other spectroscopic evidence, including an earlier infrared study,[7] has suggested that unsaturated hydrocarbons form hydrogen-bonded complexes with Bronsted sites at temperatures below that required for proton transfer. Adsorption phenomena in zeolites are of particular importance as hydrogen-bonded adsorption complexes are proposed intermediates in the catalytic transformations of hydrocarbons.[7-9]

Gorte and co-workers have recently shown that stoichiometric adsorption complexes form in several zeolites upon adsorption of methanol, 2-propanol, and 2-methyl-2-propanol.[10,11] Using temperature-programmed desorption and thermogravimetric analysis, clearly defined adsorption states with a 1:1 stoichiometry with respect to the number of Al atoms were detected in H-ZSM5, H-ZSM12, and H-mordenite for each of these adsorbates. In each case, the complexes had a similar binding energy. The results of these studies led Gorte and co-workers to conclude that the acid sites in H-ZSM5 are identical, with their presence associated with tetrahedral Al atoms of the framework.

In this contribution, we report the first variable-temperature ^{1}H MAS NMR experiments characterizing hydrogen-bonding in a zeolite. Both the structure and dynamics of hydrogen-bonded adsorption complexes formed between several adsorbates containing π bonds and the Bronsted acid proton in zeolite H-ZSM5 are discussed in detail. More importantly, this contribution is the first of its kind in that we have specifically used the Bronsted proton as our probe for adsorption phenomena and chemical exchange. Significant chemical shift changes in the Bronsted proton resonance are observed upon adsorption of stoichiometric quantities of acetylene and ethylene. The observed chemical shifts are dependent upon the loading used, reaching a near maximum downfield value at 298 K for $\geq$1 equiv of adsorbate for acetylene or ethylene. Smaller changes are observed upon adsorption of benzene, carbon monoxide, nitrogen, and ethane. For acetylene, ethylene, and carbon monoxide, a quantitative treatment of the loading-dependent chemical shifts observed at 298 K was used to calculate the respective equilibrium constants for formation of the adsorption complexes. We attribute these shifts to hydrogen-bonding interactions between the electrophilic Bronsted protons and either the π-type or n-type electrons of the adsorbate. Low-temperature MAS experiments were used to obtain the slow-exchange spectra in the presence of adsorbates as a function of loading. Here, Bronsted sites which are associated with an adsorbed molecule are clearly resolved from free Bronsted sites. Evidence for extended hydrogen-bonding networks is also provided at higher loadings of acetylene. In addition, both cross-polarization[12] and reverse cross-polarization[13] experiments at various temperatures were used to probe the dynamics of the adsorbates. These polarization-transfer experiments provide unambiguous evidence for the existence of hydrogen-bonded complexes formed specifically at the acid site.

For the cases of acetylene, ethylene, carbon monoxide, and benzene adsorption, a semiquantitative interpretation of the observed chemical shift changes is presented in terms of hydrogen-bonding contributions and shielding contributions from the magnetically anisotropic adsorbate. Both the geometries of the adsorption complexes and characteristic hydrogen-bond distances are proposed, using established rules for hydrogen-bonding in the gas phase[14] as well as known theories concerning the role of neighboring group contributions in determining the overall shielding of a proton.[15-17] The apparent similarity between hydrogen-bonded complexes in the gas phase and those formed on acid sites in H-ZSM5 suggests a method for predicting geometries and other properties of adsorption complexes in zeolites.

Experimental Section

Sample Preparation. Zeolite H-ZSM5 (UOP, Si/Al = 38) was activated to 673 K using a multistep activation procedure described previously.[18] Activated catalyst had 0.42 mmol of acid sites/g. Acetylene-$^{13}C_2$ (99% ^{13}C), acetylene-d_2 (99% D), acetylene-$^{13}C_2$-d_2 (99% ^{13}C, D), ethylene-$^{13}C_2$ (99% ^{13}C), ethylene-d_4 (99% D), and carbon monoxide-^{13}C (99% ^{13}C) were all obtained from Cambridge Isotopes. For each NMR experiment, approximately 0.06 g of activated catalyst was packed into a glass ampule, which was then evacuated to ca. 10^{-5} Torr. Following adsorption of a given loading of gas, the ampule was flame sealed and then spun in a 5-mm zirconia magic-angle spinning rotor. Experiments were performed either immediately following adsorption or following a short period of storage at 250 K to prevent either isotopic exchange or chemical reaction. In a previous in situ study of the chemistry of acetylene on H-ZSM5,[19] acetylene did not undergo chemical transformation below temperatures of ca. 350 K. With the catalyst preparation used in these experiments, ethylene was prone to oligomerization at 298 K. Therefore, it was important that only freshly prepared samples be used for the ethylene experiments. The possibility of chemical reactivity was not a concern for the other adsorbates. For experiments involving double-resonance techniques, ca. 0.18 g of catalyst was packed directly into a 7-mm rotor, and the adsorption was carried out using an improved version of the previously reported CAVERN apparatus.[18] Grooved Kel-F plugs were used to seal these samples.[20]

NMR Spectroscopy. ^{1}H and ^{13}C NMR spectra were obtained on a Chemagnetics CMX-300 spectrometer at a proton Larmor frequency of 299.7 MHz. For direct proton observation, spinning speeds of between 4 and 11 kHz were used, with most experiments conducted at ca. 6 kHz. ^{1}H NMR spectra were obtained using a 90° pulse. ^{1}H chemical shifts were referenced externally to TMS, after correction for a small, well-characterized temperature-dependent probe susceptibility effect for the spectra obtained at 123 K (0.5 ppm). The same correction factor was measured using both the zeolite in the absence of any adsorbate and a liquid chemical shift standard. The spectra reported in this contribution were obtained at either 296 or 123 K. Chemical shifts are accurate to within 0.1 ppm. Typically, eight scans were acquired using a 10-s pulse delay. For cross-polarization and reverse cross-polarization[13] experiments, spinning speeds of ca. 3–4 kHz were used to avoid attenuation of the heteronuclear dipolar interactions, and the radio-frequency field strengths were 50 kHz.

Results

Zeolite H-ZSM5 was chosen for the first investigation because, unlike some other zeolites, H-ZSM5 has only one type of Bronsted acid proton, and these sites are well isolated from one another.

(3) Ward, J. W. *Adv. Chem. Ser.* **1970**, *101*, 380.
(4) Hunger, M.; Freude, D.; Frolich, T.; Pfiefer, H.; Schwieger, W. *Zeolites* **1987**, *7*, 108.
(5) Engelhardt, G.; Michel, D. *High-Resolution Solid-State NMR of Silicates and Zeolites*; Wiley and Sons: New York, 1987; Chapter 6 and 7.
(6) Mirth, G.; Lercher, J. A.; Anderson, M. W.; Klinowski, J. *J. Chem. Soc., Faraday Trans.* **1990**, *86*, 3039.
(7) Liengme, B. V.; Hall, W. K. *Trans. Faraday Soc.* **1966**, *62*, 3229.
(8) Howard, J.; Lux, P. J.; Yarwood, J. *Zeolites* **1988**, *8*, 427.
(9) van den Berg, J. P.; Wolthuizen, J. P.; van Hooff, J. C. *J. Catal.* **1983**, *80*, 139.
(10) Gricus Kofke, T. J.; Gorte, R. J.; Farneth, W. E. *J. Catal.* **1988**, *114*, 34.
(11) Gricus Kofke, T. J.; Gorte, R. J.; Kokotailo, G. T.; Farneth, W. E. *J. Catal.* **1989**, *115*, 265.
(12) Pines, A.; Gibby, M. G.; Waugh, J. S. *J. Chem. Phys.* **1973**, *59*, 569.
(13) Crosby, R. C.; Reese, R. L.; Haw, J. F. *J. Am. Chem. Soc.* **1988**, *110*, 8550.
(14) Legon, A. C.; Millen, D. J. *Acc. Chem. Res.* **1987**, *20*, 39.
(15) Bovey, F. A. *Nuclear Magnetic Resonance Spectroscopy*; Academic Press: San Diego, 1988.
(16) McConnell, H. M. *J. Chem. Phys.* **1957**, *27*, 226.
(17) Pople, J. A.; Schneider, W. G.; Bernstein, H. J. *High Resolution Nuclear Magnetic Resonance*; McGraw-Hill: New York, 1959.
(18) Haw, J. F.; Richardson, B. R.; Oshiro, I. S.; Lazo, N. D.; Speed, J. A. *J. Am. Chem. Soc.* **1989**, *111*, 2052.
(19) Lazo, N. D.; White, J. L.; Munson, E. M.; Lambregts, M. J.; Haw, J. F. *J. Am. Chem. Soc.* **1990**, *112*, 4050.
(20) Speed, J. A.; Haw, J. F. *J. Mag. Res.* **1988**, *78*, 344.

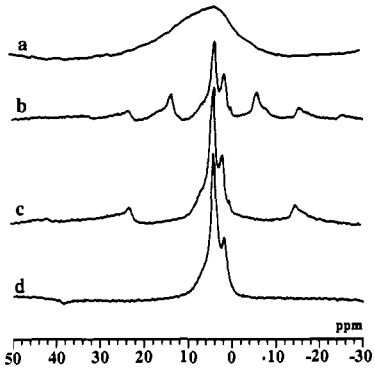

Figure 1. Proton MAS spectra of activated zeolite H-ZSM5 at various spinning speeds: (a) no sample spinning; (b) 2.5 kHz; (c) 6 kHz; (d) 11 kHz. All spectra studied were acquired at a Larmor frequency for the proton nucleus of 300 MHz. The spectra in this figure were obtained in different experiments, and direct comparisons of Bronsted peak intensity are not quantitative.

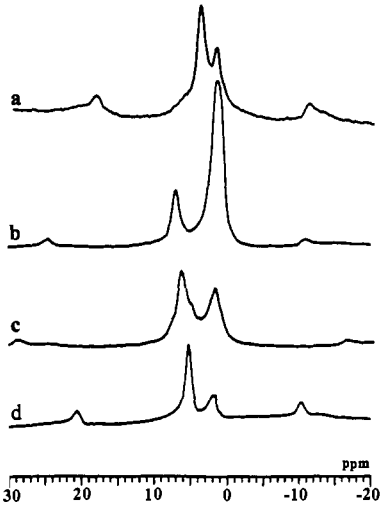

Figure 2. Proton MAS spectra of (a) H-ZSM5, (b) H-ZSM5 following adsorption of 2.0 equiv of acetylene, (c) H-ZSM5 following adsorption of 2.0 equiv of deuterated ethylene, and (d) H-ZSM5 following adsorption of 2.0 equiv of carbon monoxide.

In addition, we found that the activation of this catalyst was highly reproducible as measured by both catalytic activity and the proton NMR spectrum. Our choice of adsorbates was based upon their catalytic importance and ease of study. Furthermore, several of the adsorbates chosen had well-characterized hydrogen-bonding properties and magnetic anisotropies, and these characteristics are central to our interpretation of the induced chemical shifts.

During the course of this work, over 100 catalyst/adsorbate samples were prepared and studied, and the results reported in this contribution, to the best of our knowledge, are representative and reproducible. Proton spectra of the zeolite H-ZSM5 used in the experiments are shown in Figure 1. Figure 1a shows the static spectrum obtained in the absence of any line-narrowing techniques. Figure 1b–d shows the spectra obtained at three different spinning speeds: 2.5, 6, and 11 kHz, respectively. As can be seen, the 4.3-ppm Bronsted protons and the 2.0-ppm terminal silanol protons are clearly resolved at even moderate spinning speeds. No further improvement in resolution was achieved using combined rotational and multiple-pulse averaging techniques,[21] as was previously reported for zeolite samples.[22]

The room-temperature proton MAS spectrum obtained for H-ZSM5 is shown again in Figure 2a for comparison. Figure 2b–d shows spectra obtained following adsorption of 2.0 equiv of acetylene, 2.0 equiv of deuterated ethylene, and 2.0 equiv of carbon monoxide, respectively. The largest downfield shift observed for the Bronsted proton was seen for the acetylene case, where the acid site resonance shifted from 4.3 to 7.3 ppm. In Figure 2b, the large peak at 1.7 ppm is assigned not only to the terminal silanol hydrogens but also to the acetylene hydrogens, in agreement with both the solution-state shifts and results obtained following adsorption of acetylene-$^{13}C_2$-d_2 (spectrum not shown). Deuterated ethylene, which was used for spectral clarity in the important 4–8-ppm region, caused a downfield shift to 6.3 ppm (Figure 2c). The effect of carbon monoxide adsorption (2.0 equiv at 298 K) was to produce only a small downfield shift of the acidic resonance to 4.6 ppm, as shown in Figure 2d. No shifts in the terminal silanol resonance were observed upon adsorption of any molecules studied in this report, even at higher loadings (vide infra). The effects of these and other adsorbates on the Bronsted site chemical shift are summarized in Table I. For ease of comparison, these data are tabulated as induced chemical shift changes ($\Delta\delta$) with respect to the unperturbed acid site resonance taken as 0.

The loading-dependent chemical shifts reported in Table I suggest exchange-averaging at 298 K. The shifts induced by either acetylene or ethylene approach their respective maximum downfield shifts at ca. 1.0 equiv or greater, whereas the maximum shift observed at room temperature for carbon monoxide occurs at greater than 6.0-equiv loading. At 2.0 equiv of adsorbate, acetylene induces a downfield shift in the Bronsted resonance 1.0 ppm greater than that for ethylene and 2.0 ppm greater than that for carbon monoxide. In Figure 3 are shown graphs of the Bronsted acid site chemical shift as a function of acetylene loading

Table I. Induced Chemical Shift Changes ($\Delta\delta$) for the Bronsted Acid Hydrogen on H-ZSM5 as a Function of Adsorbate Loading

adsorbate	loading (equiv)	$\Delta\delta$ at 298 K	$\Delta\delta$ at 123 K
C_2H_2/C_2D_2	3.0	3.0	4.1
	2.0	3.0	3.9
	1.0	2.4	3.5
	0.5	1.4	3.5, 0.0[a]
C_2H_4/C_2D_4	3.0	2.0	2.7
	2.0	2.0	2.7
	1.0	1.8	2.7
	0.5	0.9	2.7, 0.0[a]
C_6H_6	2.0	0.5	–[b]
C_2H_6	2.0	0.3	0.6
CO	0.5	0.3	0.7
	1.0	0.6	1.8
	2.0	1.0	1.8
	4.0	1.2	1.8
	>6.0	1.5	1.8
N_2	2.0	0.3	0.3

[a] Two chemical shifts are reported for spectra that show clearly resolved slow-exchange features. [b] See text for variable-temperature results.

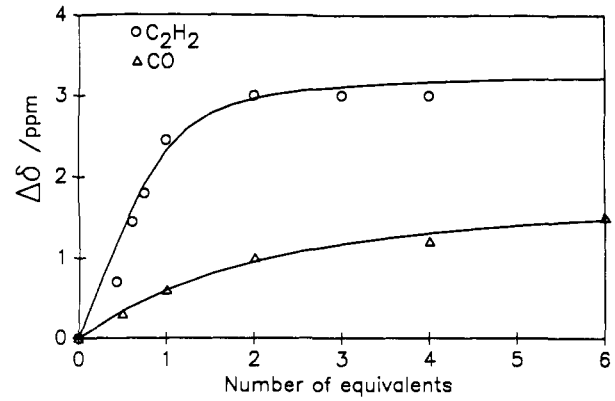

Figure 3. Graph of Bronsted site proton chemical shift at 298 K vs number of equivalents of acetylene (top) and carbon monoxide (bottom) adsorbed. Experimental data are indicated by circles and triangles. Fits to the experimental data using values of K_{eq} = 7 equiv^{-1} for acetylene and 0.7 equiv^{-1} for carbon monoxide are given by solid lines.

(21) Gerstein, B. C. *Philos. Trans. R. Soc. London* **1981**, *A299*, 521.
(22) Dec, S. F.; Bronniman, C. E.; Wind, R. A.; Maciel, G. E. *J. Magn. Reson.* **1989**, *82*, 454.

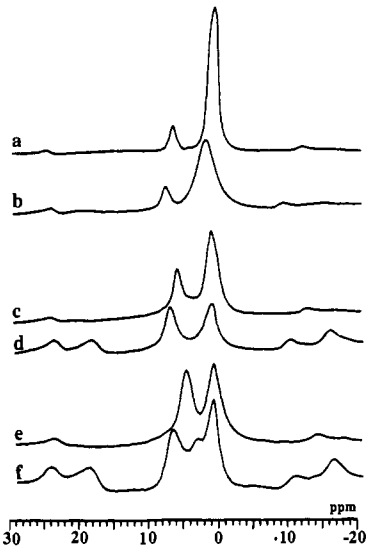

Figure 4. Proton MAS spectra obtained following room-temperature adsorption of (a) 3.0 equiv of acetylene on H-ZSM5 with the spectrum acquired at 298 K, (b) same as part a with the spectrum acquired at 123 K, (c) 1.0 equiv of acetylene at 298 K, (d) same as part c with the spectrum acquired at 123 K, (e) 0.5 equiv of acetylene at 298 K, and (f) same as part e with the spectrum acquired at 123 K. Quantitative comparisons of signal intensity are correct only for the spectra obtained for the same loading, i.e., spectra a and b.

and carbon monoxide loading, respectively. In the Discussion, we will show that these curves can be fit (Figure 3, solid lines) to determine the values of the equilibrium constants characterizing the formation of the hydrogen-bonded complexes.

Variable-temperature ^1H MAS NMR experiments were performed on a number of adsorbates and loadings. The acetylene and ethylene cases were studied in the greatest detail. These experiments confirm the existence of a standard two-site exchange problem. Figure 4a shows the proton spectrum obtained at 298 K following adsorption of 3.0 equiv of acetylene. Similar spectra for 1.0 and 0.5 equiv are shown in parts c and e, respectively, of Figure 4. The Bronsted site shift decreases from 7.3 to 6.7 to 5.7 ppm as the loading decreases from 3.0 to 1.0 to 0.5 equiv. When the 3.0-equiv sample was cooled to 123 K, the acidic resonance shifted further downfield to 8.4 ppm (Figure 4b). A smaller shift to 7.8 ppm was observed in the 1.0-equiv case as shown in Figure 4d. For a 2.0-equiv sample (spectrum not shown), an intermediate shift to 8.2 ppm was observed at 123 K. In addition, the signal for the acetylene protons, normally at 1.7 ppm at 298 K, also shifted downfield to 2.4 ppm at 123 K for the 2.0- and 3.0-equiv-loading samples.

The most interesting spectrum was that obtained for the 0.5-equiv loading of acetylene at 123 K shown in Figure 4f. Here, slow exchange with respect to the free acid site and the complexed site is obvious and the single 5.7-ppm peak observed at 298 K is split into a peak at 4.3 ppm and a peak at 7.8 ppm, respectively. Separate low-temperature experiments on samples prepared with ca. 0.2-equiv and ca. 0.8-equiv loadings confirmed the expected increase or decrease in the intensities of the free acid site peak at 4.3 ppm and the peak assigned to the complex at 7.8 ppm (spectra not shown).

Similar spectra are shown for deuterated ethylene in Figure 5. For 1.0 and 0.5 equiv (Figure 5a,c), the room-temperature Bronsted site chemical shifts were 6.1 and 5.4 ppm, respectively. Again, a limiting downfield shift value of 6.4 ppm was reached at $\geq$2.0 equiv of ethylene (spectra not shown). The spectra obtained for the 1.0-equiv sample at 123 K, Figure 5b, shows a 7.0-ppm peak for the shifted Bronsted site. The same 7.0-ppm shift was also observed for a 3.0-equiv sample at 123 K (see Table I). However, in contrast to the acetylene case, the slow-exchange spectrum for the 0.5-equiv sample (Figure 5d) also shows a peak at 7.0 ppm for the complexed acid site in addition to the free acid site at 4.3 ppm. For ethylene loadings in excess of 1.0 equiv,

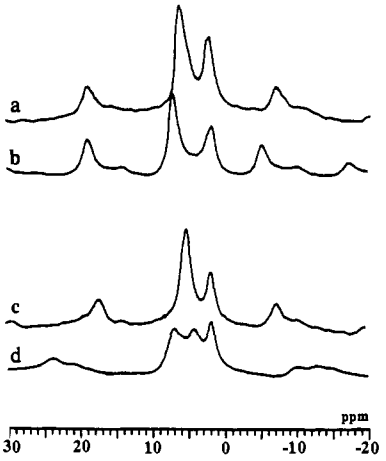

Figure 5. Proton MAS spectra obtained following room-temperature adsorption of (a) 1.0 equiv of deuterated ethylene at 298 K, (b) same as part a with the spectrum acquired at 123 K, (c) 0.5 equiv of deuterated ethylene and 298 K, and (d) same as part c with the spectrum acquired at 123 K.

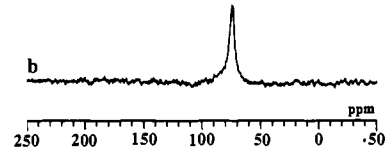

Figure 6. 75-MHz ^{13}C-observed cross-polarization MAS spectra for ca. 1 equiv of deuterated acetylene adsorbed on H-ZSM5 acquired at (a) 298 K and (b) 123 K. Two hundred scans were acquired using a 2-ms contact time and a 2-s pulse delay.

additional downfield shifts in the acid site chemical shift were not observed at 123 K. Comparisons of chemical shifts versus loadings at both 298 and 123 K for acetylene and ethylene, as well as the other adsorbates studied, are given in Table I.

The observation that one peak at room temperature splits into two clearly resolved peaks in the low-temperature spectra for both acetylene and ethylene at loadings of less than 1 equiv provides compelling evidence for the existence of hydrogen-bonded adsorption complexes between these molecules and the Bronsted acid site proton. If, in the proposed complex, the Bronsted acid site proton and the carbon of the adsorbed molecule are sufficiently close, the possibility of transferring polarization from the acidic proton to the carbons of the adsorbate exists. Polarization-transfer techniques, such as cross-polarization,[12] should provide additional confirmation of the existence of the proposed complex. Using 1.0 equiv of acetylene-$^{13}C_2$-d_2 adsorbed on H-ZSM5, an attempt was made to obtain a ^{13}C cross-polarization spectrum at 298 K. As seen in Figure 6a, no signal was observed. Since the proton spectra described above for acetylene adsorption indicated that the acetylene was in the fast-exchange motional regime at room temperature, sufficient averaging of the heteronuclear dipolar interactions due to the motion might be expected to preclude efficient polarization transfer. However, at 123 K, a $^1H \rightarrow {}^{13}C$ cross-polarization signal at the expected chemical shift of 77 ppm was easily obtained using the same parameters and is shown in Figure 6b. Since the deuterated adsorbate had no directly attached protons, the proton polarization must have come from the protons of the zeolite lattice. Although a carbon-observed cross-polarization experiment at low temperatures is consistent with complex formation, it does not identify which zeolite protons are coupled to the carbons of the adsorbate via dipole–dipole interactions.

Recently, Haw and co-workers reported a variant of the standard cross-polarization experiment which is useful for assigning resonances to specific proton environments.[13] That experiment involves transferring polarization from the low-γ nucleus to the proton, i.e., a $^{13}C \rightarrow {}^1H$ cross-polarization experiment, where the

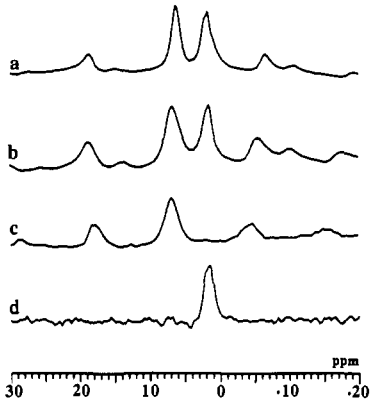

Figure 7. Proton MAS spectra obtained using the same sample as in Figure 6: (a) single-pulse spectrum at 298 K; (b) same as in part a, but at 123 K; (c) proton-observed reverse cross-polarization spectrum of the sample in part b at 123 K; (d) proton-observed reverse cross-polarization spectrum obtained for protonated acetylene on H-ZSM5 at 298 K.

proton is the observed nucleus. This particular experiment would clearly indicate which zeolite protons were within several angstroms of the carbon-13 nuclei of the adsorbate. The proton MAS spectra of 1.0 equiv of C_2D_2 on H-ZSM5 at 298 and 123 K are shown in Figure 7a,b. These spectra are analogous to those shown previously in Figure 4. As before, there are two peaks, the downfield Bronsted proton and the upfield terminal silanol resonance. If the complexed acetylene is associated with the Bronsted proton only, cross-polarization from the carbon-13 spins to the proton spins should give only one peak at the same chemical shift observed for the acidic proton in Figure 7b. Indeed, this was the experimental observation. The $^{13}C \rightarrow {}^{1}H$ reverse cross-polarization spectrum obtained at 123 K is shown in Figure 7c. *This provides unambiguous evidence of an adsorption complex formed between acetylene and specifically the Bronsted acid site.* For completeness, the reverse cross-polarization spectrum for protonated acetylene on H-ZSM5 at 298 K is shown in Figure 7d. Here, only one peak at 1.7 ppm for the acetylene protons is observed, as is expected since the acetylene is in the fast motional regime at that temperature.

The use of C_2D_2 and C_2D_4 was motivated by the need to make accurate chemical shift assignments, but their study also allowed us to make some qualitative observations regarding $^{1}H-^{2}H$ scrambling with the acid site. In general, we found that, for acetylene adsorbed on H-ZSM5, exchange occurred at room temperature over a period of several days. Ethylene, however, underwent isotopic exchange over a period of a few hours with the catalyst preparation used in this study. As such, all of our samples were run immediately following preparation or after a short period of storage at 250 K.

In our attempts to investigate the hydrogen-bonding properties of benzene with a course of study analogous to that used for acetylene and ethylene, we observed that isotopic exchange occurred at room temperature over a time scale of a few minutes or less. In Figure 8 is shown a series of ^{1}H MAS spectra obtained following cryogenic adsorption of 2.0 equiv of benzene-d_6 on H-ZSM5 and subsequent heating from 173 K to ambient temperature. With this method of sample preparation, the benzene-d_6 is initially frozen outside the zeolite channels, and it enters the zeolite as the temperature is raised. In the bottom spectra of Figure 8 (173 K), only a very small peak at 7.5 ppm is seen, indicating that relatively no isotopic exchange had occurred. Again, the acidic site peak was at 4.3 ppm and the external silanol peak was at 2.0 ppm. Upon raising the temperature to 263 K, an additional peak at 5.1 ppm became resolved. At 293 K and above, the 4.3-ppm and the 5.1-ppm peaks were no longer clearly resolved; they were replaced by a single resonance at 4.8 ppm. Although the melting point of benzene is 278 K, it has significant vapor pressure at 253 K and above (e.g., 12 Torr at 263 K) to allow it to enter the zeolite channels. We therefore assign the peak at 5.1 ppm to Bronsted acid sites hydrogen-bonded to a

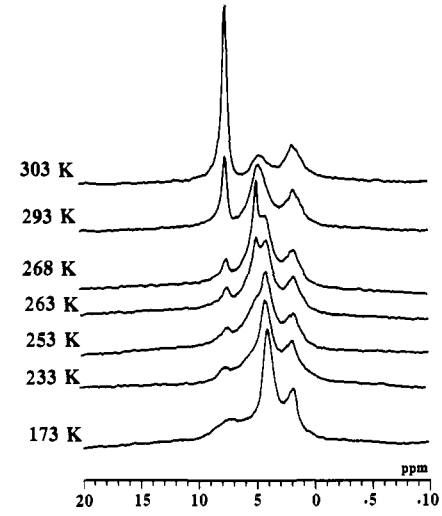

Figure 8. Proton MAS spectra showing the formation of an adsorption complex followed by proton–deuterium exchange as a sample of frozen benzene-d_6 on H-ZSM5 is heated from 173 K to ambient temperature.

benzene molecule. Free and complexed acid sites were clearly resolved at 263 and 268 K. Label exchange between benzene-d_6 and the Bronsted site in the zeolite became rapid when the sample temperature was raised to 293 K, and a proton signal for benzene grew in at a chemical shift of 7.5 ppm at the expense of the signal for the Bronsted site.

Discussion

The results of this study are discussed in several sections for convenience. The loading-dependent chemical shifts observed for the Bronsted site in the presence of acetylene, ethylene, and carbon monoxide are used to determine equilibrium constants for the formation of the hydrogen-bonded complexes. This analysis is significant in that it provides information concerning the relative strengths of the hydrogen bonds, independent of the mechanism of the induced chemical shifts. Secondly, the geometries of analogous hydrogen-bonded dimers formed in the gas phase are introduced to establish a basis for the geometries of the complexes formed at the Bronsted site in H-ZSM5. Hydrogen-bond force constants and hydrogen-bond distances for gas-phase dimers of HCl and the molecules used in this study are introduced, and their relevance to our NMR results is discussed. The observed chemical shift behavior for the Bronsted proton in the presence of the molecules used in this study is then interpreted using a chemical shift model which contains contributions from hydrogen-bonding effects and neighboring group anisotropy effects. The relationship between the two contributions to the chemical shifts of the Bronsted proton, the equilibrium constants, and gas-phase force constant data is explained. We discuss the proposed geometries of the adsorption complexes with regard to our model for the observed chemical shift. Finally, extended hydrogen-bonding networks and hydrogen-deuterium scrambling between adsorbates and the Bronsted site are addressed.

Complex Formation Equilibria. The loading-dependent $\Delta\delta$ values for the Bronsted site peak following acetylene and carbon monoxide adsorption at 298 K are given in Table I. Graphs of the observed acid site chemical shift versus loading of each adsorbate are shown separately in Figure 3. Resembling a titration curve, the plots are a function of the equilibrium constant for the formation of the hydrogen-bonded complexes between the acid site and acetylene or carbon monoxide. Since the adsorbates are in fast exchange at 298 K, the observed chemical shift is the population-weighted average shift given by eq 1,

$$\Delta\delta_{obsd} = [ADS\text{---}HO\text{-}Z]\Delta\delta_{max} \quad (1)$$

where $\Delta\delta_{obsd}$ is the observed Bronsted site chemical shift, [ADS---HO-Z] is the equilibrium concentration of the adsorption complex normalized to a maximum concentration of unity, and $\Delta\delta_{max}$ is the observed chemical shift change in the limit of complete

complexation of the Bronsted hydrogen. $\Delta\delta_{max}$ can in principle be determined in one of three ways: by treating it as a free parameter in fits of plots like those in Figure 3; from $\Delta\delta$ values at room temperature for samples with very high loadings; or from $\Delta\delta$ values obtained for the complexed Bronsted proton at low temperature in the slow-exchange limit. Because of the possibility of temperature-dependent chemical shifts or extended hydrogen-bonding networks at high loadings, it is probably best to treat it as a free parameter (although we show later that all three methods are in close agreement).

The equilibrium constant, K, for formation of the complex is defined explicitly in this case by the following equation:

$$K = \frac{[\text{ADS}\cdots\text{HO-Z}]}{[\text{ADS}][\text{Z-OH}]} \tag{2}$$

where [ADS] is the equilibrium concentration of free adsorbate and [Z-OH] is the equilibrium concentration of free acid site. If we express the concentrations in equivalents, the following equations apply:

$$[\text{Z-OH}] + [\text{ADS}\cdots\text{HO-Z}] = 1 \tag{3}$$

$$C_{ads} = [\text{ADS}] + [\text{ADS}\cdots\text{HO-Z}] \tag{4}$$

where C_{ads} is the analytical concentration of the adsorbate in equivalents, i.e., the number of equivalents added to the zeolite as opposed to the actual concentration of uncomplexed adsorbate. Using the above equations, it can be shown that the expression for the observed change in chemical shift is a function of the equilibrium constant and the amount of adsorbate introduced (in equivalents) is given by eq 5. For the case of acetylene and

$$\Delta\delta_{obsd} = \Delta\delta_{max}\left[\frac{\left(1 + C_{ads} + \frac{1}{K}\right) - \sqrt{\left(1 + C_{ads} + \frac{1}{K}\right)^2 - 4C_{ads}}}{2}\right] \tag{5}$$

ethylene adsorption, the experimental data were fit using a wide range of K values, but reasonable fits were obtained only when values of K between 7 and 10 equiv^{-1} were used. The simulated fit using K = 7 equiv^{-1} and $\Delta\delta_{max}$ = 3.3 ppm is shown by the smooth curve in Figure 3, and it is in excellent agreement with the experimental points. This value of $\Delta\delta_{max}$ is consistent with the maximum shift observed at room temperature of 3.0 ppm and the slow-exchange value of 3.5 ppm obtained from the 0.5-equiv sample at 123 K. A similar treatment for ethylene using K between 7 and 10 equiv^{-1} and $\Delta\delta_{max}$ = 2.2 ppm fits experimental data closely for variable loadings at 298 K (data not shown). Again, the $\Delta\delta_{max}$ of 2.2 ppm for ethylene adsorption is in agreement with the maximum shift observed at 298 K (2.0 ppm) and 123 K (2.7 ppm). For carbon monoxide the experimental data were fit using K = 0.7 equiv^{-1} and $\Delta\delta_{max}$ = 1.8 ppm. This $\Delta\delta_{max}$ was identical to the experimental shift value observed for CO at 123 K. As can be seen in Figure 3, the agreement is excellent. The significance of the values of K as determined from the loading-dependent chemical shifts of the Bronsted proton in the presence of acetylene, ethylene, or carbon monoxide is that they reflect the strengths of the hydrogen bond formed at the acid site.

Changes in the line shape of the Bronsted proton peak upon adsorption or errors in the measurement of chemical shifts could result in errors in the above treatment of equilibrium constants. In reviewing the Bronsted peak line shape in Figues 1–8, it is clear that the only change that occurs upon adsorption is in the isotropic chemical shift, not the line shape. Indeed, the line shape is in every way consistent with previously reported spectra of H-ZSM5:[4,5] an inhomogeneously broadened line shape resulting from a distribution in microcrystalline environments. Measurements of ^{1}H NMR chemical shifts in zeolites obtained using MAS have been reviewed recently by Engelhardt,[5] and excellent consistency in the chemical shifts for H-ZSM5 obtained in many laboratories is observed. Any systematic errors in chemical shift measurements reported in this study are compensated for, since all calculations are based on $\Delta\delta$ values, not absolute chemical shifts. If one assumes an error in $\Delta\delta$ of 0.1 ppm and a 0.1-equiv uncertainty in the loadings for a single point, this propagates as a ca. 40–50% error in the calculation of K. This is clearly a worst case estimate, as five or more data points are used in fits like those in Figure 3. We estimate that the uncertainty in the reported K values is ca. 20%.

Table II. Comparison of Gas-Phase Stretching Force Constants, k, and Bond Distances, r, for Base-HCl Dimers to Observed $\Delta\delta$ Values at 298 and 123 K for 2.0 equiv of Base

base	k (N/m)[a]	r(corr)[a]	$\Delta\delta_{298K}$	$\Delta\delta_{123K}$
C_2H_2	6.4	2.41	3.0	3.8
C_2H_4	5.9	2.44	2.1	2.7
C_2H_6	–[b]	–[b]	0.3	0.3
C_6H_6	8.0	2.35	0.5	0.8[c]
CO	3.9	2.41	1.0	1.8
N_2	2.5	2.42	0.3	0.3

[a] Compiled from refs 24–30; see footnote 36. [b] We were unable to locate a report of the ethane–HCl system. [c] This value was assigned from the 253 K spectrum; see text.

It might be assumed that the magnitudes of the induced changes in the chemical shift of the Bronsted proton upon formation of the hydrogen-bonded complexes should reflect the relative strengths of the hydrogen bonds formed. Even though the equilibrium constant values for acetylene and ethylene complexation are identical, their respective $\Delta\delta_{max}$ values differ by ca. 1.0 ppm. There must be another contribution to the chemical shift besides the electronic effect due to hydrogen-bond formation. The small shift induced by benzene is clearly inconsistent with the large force constant for the analogous gas-phase complex. In order to develop a theory for the chemical shifts observed in this study, we first propose geometries for these complexes.

Hydrogen-Bonding Geometries. One might reasonably assume that the geometries of hydrogen-bonded complexes formed at the acid site in the zeolite may be modeled by analogous gas-phase dimers with an acid such as HCl. Numerous gas-phase rotational–vibrational experiments have confirmed the following rules concerning hydrogen-bonded dimer geometries:[14]

1. The axis of the HX molecule coincides with the axis of a nonbonding electron pair of the base (e.g., CO).
2. The axis of the HX molecule intersects the internuclear axis of the atoms forming the π bond and is perpendicular to the plane of symmetry of the π bond of the base (e.g., C_2H_2, C_2H_4, and C_6H_6).
3. If the base has both nonbonding electron pairs and π-bonding pairs, hydrogen-bonding will occur preferentially through the nonbonding pairs.

Comparisons of the hydrogen-bond stretching force constants and hydrogen-bond distances for dimers of molecules used in this study and HCl are shown in Table II. It is important to note that although the bond stretching force constant, k, varies considerably among the dimer series, the bond distance, r, is constant at ca. 2.4 Å with less than a 0.1-Å variation.

Assuming that the geometries of the hydrogen-bonded complexes in the zeolites obey the above rules, we propose the following structure for the complexes of acetylene and ethylene, where we have used Rabo's resonance model view of the acid site[1] in the zeolite.

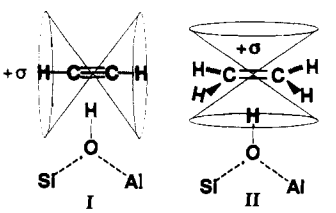

Similarly, the Bronsted proton would bond to the π cloud of benzene along the 6-fold axis, with the ring plane perpendicular to the hydrogen-bond axis. Carbon monoxide would presumably

be hydrogen-bonded through the nonbonding electron pair on the carbon. The shaded and non-shaded regions in the above structure refer to the signs of the bond magnetic susceptibility anisotropy associated with the adsorbate molecule. The significance of this magnetic property will be apparent later in the Discussion.

One possible objection to our model is that the gas-phase structures with which we make some analogy are very unstable with respect to rapid dissociation and exchange, and as such must be studied in the gas phase at rotational temperatures of less than ca. 10 K. However, even at 123 K, our zeolitic adsorption complexes are also undergoing rapid dissociation and reassociation. The observation of a slow-exchange spectrum at 123 K merely implies a lower limit on the lifetime of the complexes of the order of a few milliseconds. Furthermore, it is reasonable that the stabilities of the complexes in the zeolite are higher than the stabilities of the corresponding gas-phase complexes on entropic grounds, since there are fewer degrees of freedom available to the adsorbate molecule within the confined channels of the zeolite upon dissociation of the complex.

Chemical Shift Model. The effects of hydrogen-bonding on proton chemical shifts have been extensively studied. To a first approximation, the formation of a hydrogen bond is accompanied by a downfield shift in the proton resonance due to the polarization of the O–H bond by the electric field gradient of the adsorbate.[23] The inconsistencies mentioned above in comparing $\Delta\delta_{max}$ values with equilibrium constants and k values may be understood using a chemical shift model in which the change in chemical shift ($\Delta\delta_{max}$) due to hydrogen-bonding is treated as the sum of two components.

$$\Delta\delta = \Delta\delta_{local} + \Delta\delta_{nga} \quad (6)$$

$\Delta\delta_{local}$ is the contribution from electronic effects due to hydrogen-bonding. The second term is the contribution from the magnetic anisotropy of the adsorbate molecule, and this effect is traditionally called a neighboring group anisotropy contribution. Ring current shifts are a familiar example of a neighboring group anisotropy contribution, and a similar effect accounts for the otherwise anomalously magnetic properties and, as such, could further alter the shielding of the Bronsted proton upon formation of the hydrogen-bonded complex. These neighboring group effects have been extensively studied, and the influence of neighboring group anisotropy and the special case of ring current effects on proton NMR spectra has been the subject of recent reviews.[15,24] These effects may be analyzed quantitatively. Early in the development of chemical shift theory, both McConnell[16] and Pople[17] independently showed that the neighboring group may be modeled by a point magnetic dipole, the moment of which is anisotropic in accordance with the diamagnetic susceptibility. This contribution to the overall shift of the nucleus of interest may be expressed as

$$\Delta\delta_{nga} = -\frac{10^6}{12\pi r^3}(\chi_{\parallel} - \chi_{\perp})(1 - 3\cos^2\theta) \quad (7)$$

where r is the hydrogen-bond distance, $(\chi_{\parallel} - \chi_{\perp})$ is the anisotropy of the bond magnetic susceptibility of the neighboring group, and θ is the angle between the hydrogen-bond axis and the neighboring group bond axis. θ was taken to be 90° based upon the known equilibrium gas-phase geometries.[14,25-30] Since changes in shielding are measured for the acidic proton upon complex formation and the susceptibility anisotropies are known for several of the adsorbates, the hydrogen-bond distance may be calculated.

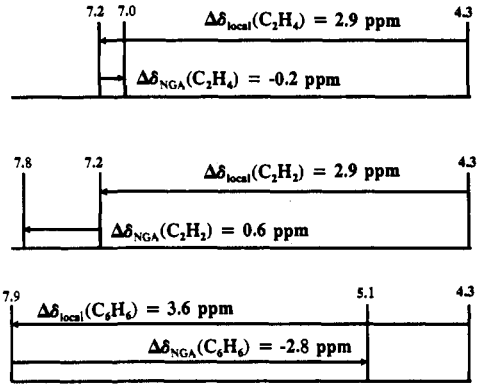

Figure 9. Schematic diagram showing our interpretation of the observed chemical shift of the Bronsted proton following adsorption of either ethylene, acetylene, or benzene. As discussed in the text, the two contributions are the local or hydrogen-bond effect and the neighboring group magnetic anisotropy effect.

Using susceptibility data compiled from the literature,[31-34] eq 6 was formulated for the acetylene and ethylene complexes as follows:

$$\Delta\delta_{local}(C_2H_2) + \Delta\delta_{nga}(C_2H_2) = 3.5 \text{ ppm}$$

$$\Delta\delta_{local}(C_2H_4) + \Delta\delta_{nga}(C_2H_4) = 2.7 \text{ ppm}$$

We assume that $\Delta\delta_{local}$ is the same for both acetylene and ethylene on the basis of their similar values for the equilibrium constants and gas-phase force constants. Simultaneous solution yields $\Delta\delta_{local}$ as 2.94 ppm and r = 2.5 Å.[35,36] The slow-exchange shifts for the Bronsted proton at 123 K were used in the above calculation for the shift of the complexed proton. The r value obtained is consistent with those shown in Table I for gas-phase dimers with HCl, and the assumption that acetylene and ethylene have similar bond distances is reasonable on the basis of the bond distances in Table I. Furthermore, this hydrogen-bond distance is consistent with the adsorbate being positioned near the center of the zeolite channel, which has a diameter of ca. 5.5 Å.[1]

If the calculation is repeated with the assumption of a 0.1-ppm uncertainty in the chemical shift, values for the hydrogen-bond distance r range from 2.34 to 2.78 Å, and $\Delta\delta_{local}$ ranges from 2.9 to 3.0 ppm. We do not maintain that this is the preferred method for determining hydrogen-bonding distances in zeolites, only that the Bronsted proton chemical shift reflects the structure of the π-bonded complexes in a semiquantitative way. Although the point dipole model used in the calculation is a classical model, it has been shown in other work that the model provides results which agree closely with experimental data.[24] Recently, Kazansky and co-workers have used quantum chemical methods on model clusters to study the adsorption complex formed between ethylene and the acidic proton in zeolites.[37] Although the hydrogen-bond distance determined in that study (2.22 Å) is slightly less than the range we report, the geometry of the adsorption complex is almost identical to that which we propose on the basis of our NMR data.

The anomalously small Bronsted proton shift observed upon adsorption of benzene may also be treated using the Waugh–Fessenden–Johnson–Bovey semiempirical classical model[38] for

(23) Davis, J. C., Jr.; Deb, K. K. *Adv. Magn. Reson.* **1970**, *4*, 201.
(24) Haigh, C. W.; Mallion, R. B. *Prog. Nucl. Magn. Reson. Spectrosc.* **1980**, *13*, 303.
(25) Read, W. G.; Flygare, W. H. *J. Chem. Phys.* **1982**, *76*, 2238.
(26) Shea, J. A.; Flygare, W. H. *J. Chem. Phys.* **1982**, *76*, 4857.
(27) Legon, A. C.; Aldrich, P. D.; Flygare, W. H. *J. Chem. Phys.* **1981**, *75*, 625.
(28) Aldrich, P. D.; Legon, A. C.; Flygare, W. H. *J. Chem. Phys.* **1981**, *75*, 2126.
(29) Read, W. G.; Campbell, E. J.; Henderson, G. *J. Chem. Phys.* **1983**, *78*, 3501.
(30) Soper, P. D.; Legon, A. C.; Flygare, W. H. *J. Chem. Phys.* **1981**, *74*, 2138.
(31) Harris, R. K. *Nuclear Magnetic Resonance Spectroscopy*; Longman Scientific and Technical: London, 1986; Table 8-7.
(32) Cheng, C. L.; Murthy, D. S.; Ritchie, G. L. *Mol. Phys.* **1971**, *22*, 1137.
(33) Kato, Y.; Fujimoto, Y.; Saika, A. *Chem. Phys. Lett.* **1972**, *13*, 453.
(34) Bogaard, M. P.; Buckingham, A. D.; Corfield, M. G.; Dunmur, D. A.; White, A. H. *Chem. Phys. Lett.* **1971**, *12*, 558.
(35) This treatment is strictly correct for single and triple bonds due to symmetry. Double bonds in principle have three unique principal components in the susceptibility tensors, but for the case of a carbon–carbon double bond, two are identical, and eq 7 applies.
(36) In making these comparisons, the center of mass distances in refs 25–30 were corrected to hydrogen-bond distances using a bond distance for HCl of 1.28 Å as reported therein.
(37) Kazansky, V. B. *Acc. Chem. Res.* **1991**, *24*, 379.

determining the ring current, i.e., neighboring group, contribution to the overall shielding of the Bronsted proton. Assuming a similar value of r = 2.5 Å as was determined from the acetylene and ethylene shifts, the isoshielding treatment of Johnson and Bovey predicts that, for the geometry proposed earlier, the neighboring group contribution to the overall shift will be −2.8 ppm. The observed chemical shift for the complexed Bronsted proton was 5.1 ppm, and a $\Delta\delta_{local}$ value of 3.6 ppm was calculated by difference (see Figure 9).

The observed $\Delta\delta_{max}$ value for CO at 123 K, 1.8 ppm, is significantly smaller than the corresponding values for either acetylene or ethylene. This reflects the relative values of both $\Delta\delta_{local}$ and $\Delta\delta_{nga}$. Again, assuming that equilibrium constants and the gas-phase force constants can be used to predict the electronic contribution to the observed shifts, a smaller value of $\Delta\delta_{local}$ is expected for the adsorption of CO. Furthermore, application of the rules for predicting the geometries of gas-phase complexes suggests that CO should hydrogen-bond using the unshared electron pair on the carbon directed out along the CO bond axis. We have been unable to locate magnetic susceptibility anisotropy data for CO, but the neighboring group contribution to the observed shift of the Bronsted proton induced by this geometry should be upfield, further contributing to the relatively low $\Delta\delta_{max}$ value observed for CO adsorption.

A schematic representation of our model for the chemical shifts of ethylene, acetylene, and benzene is shown in Figure 9. This model yields $\Delta\delta_{local}$ values which are consistent with the relative ordering of equilibrium constants and/or force constants for analogous dimers. Furthermore, the structures of complexes predicted by neighboring group contributions to the chemical shift model are in agreement with the proposed geometries.

Extended Hydrogen-Bonding Networks. The low-temperature $\Delta\delta$ values observed for the Bronsted proton in the presence of different loadings of acetylene (see Table I) are unusual in that the Bronsted resonance shifts farther downfield with increased acetylene loading, reaching a maximum shift of 8.4 ppm at 123 K for a 3.0-equiv loading. Furthermore, for the 2.0- and 3.0-equiv samples (but not the 1.0-equiv sample), the acetylene proton resonance also shifted downfield from 1.7 to 2.4 ppm at 123 K. It is known that acetylene protons are weakly acidic.[39] We attribute these shift characteristics to the formation of extended hydrogen-bonded networks at the acid site at low temperature. This type of extended complex would account for both the decreased shielding of the zeolite Bronsted proton and the acetylenic proton. It is important to note that this behavior was observed only at loadings of greater than 1.0 equiv. In contrast, ethylene, which is not known to undergo intermolecular hydrogen-bonding, did not exhibit loading-dependent shifts of the acidic proton resonance in the spectra obtained at 123 K.

Isotopic Exchange. Finally, we comment on the experimental observations concerning deuterium–hydrogen exchange. As mentioned earlier, isotopic exchange occurred much more slowly with acetylene than for ethylene, and it occurred the fastest with benzene. In Figure 8, the variable-temperature spectra indicate that the rate of isotopic exchange for benzene-d_6 on H-ZSM5 increases greatly above 268 K. It appears that the formation of the hydrogen-bonded complex with the Bronsted site facilitates this exchange. As such, it is possible that this type of complex is the first formed species in catalytic transformations that occur in zeolites. Furthermore, the opportunity to measure isotopic exchange rates for catalytically significant adsorbates, such as benzene, in experiments analogous to Figure 8, suggests a method for quantifying the relative kinetic acidities of different zeolite catalysts.

Conclusions

We have shown that the chemical shift of the acidic Bronsted proton in zeolite H-ZSM5 is extremely sensitive to the amount and type of adsorbate introduced. The changes in chemical shift are consistent with the formation of hydrogen-bonded adsorption complexes, with the electrophilic Bronsted hydrogen-bonded to either the π cloud or nonbonding electrons of the adsorbate. The specificity of hydrogen-bonding between the adsorbate and the Bronsted site was confirmed by variable-temperature MAS experiments as well as cross-polarization and reverse cross-polarization techniques. At 298 K, the adsorbates were found to be in fast exchange, whereas at 123 K, slow-exchange behavior with respect to the Bronsted proton chemical shift was observed. We have shown that loading-dependent chemical shift changes can be interpreted in terms of the complex formation equilibrium constant, independent of the mechanism of the induced chemical shifts. The equilibrium constants at 298 K were determined to be ca. 6–9, 6–9, and 0.6–0.9 equiv^{-1} for acetylene, ethylene, and carbon monoxide, respectively. These values are consistent with trends in the relative force constant of analogous gas-phase dimers.

The maximum observed chemical shift changes upon adsorption do not correlate with the strength of the hydrogen-bonding interaction as either measured in terms of the equilibrium constant or predicted on the basis of gas-phase force constants. We have introduced a chemical shift theory that satisfactorily accounts for this observation in terms of an electronic contribution related to the strength of the hydrogen bond and a magnetic term related to the anisotropic susceptibility of the adsorbate and the geometry of the complex. The overall agreement obtained with this model suggests that the hydrogen-bonded complexes in the zeolite are indeed similar to analogous gas-phase dimers. Similar results for the geometry of hydrogen-bonded complexes obtained recently using quantum chemical methods further support this model.

The ability to measure isotopic exchange rates between acid sites in zeolites and catalytically relevant adsorbates suggests a new strategy for characterizing acidity in zeolites.

Acknowledgment. This work was supported by the National Science Foundation (Grant CHE-8918741). The Department of Defense provided funds for the purchase of the NMR spectrometer. J.L.W. is a Dow Chemical graduate fellow. L.W.B. is an IUCCP graduate fellow. We thank Michael Bothwell for assistance in preparing the art work.

Registry No. HC≡CH, 74-86-2; H_2C=CH_2, 74-85-1; CO, 630-08-0; C_6H_6, 71-43-2; H_3CCH_3, 74-84-0; N_2, 7727-37-9.

(38) Johnson, C. E., Jr.; Bovey, F. A. *J. Chem. Phys.* **1958**, *29*, 1012.
(39) March, J. *Advanced Organic Chemistry*; McGraw-Hill: New York, 1985; p 154.